Published in final edited form as:
Chembiochem. 2014 September 22; 15(14): 2125–2131. doi:10.1002/cbic.201402258.

Functional chromatography reveals three natural products that target the same protein with distinct mechanisms of action

MinJin Kang[a,†], **Tongde Wu**[a,†], **E. M. Kithsiri Wijeratne**[b], **Eric C. Lau**[a], **Damian J. Mason**[a], **Celestina Mesa**[a], **Joseph Tillotson**[a], **Donna D. Zhang**[a], **A. A. Leslie Gunatilaka**[b], **James J. La Clair**[c], and **Eli Chapman**[a]

Eli Chapman: chapman@pharmacy.arizona.edu

[a]College of Pharmacy, Department of Pharmacology and Toxicology, University of Arizona, Tucson, AZ 85721-0207, United States

[b]Southwest Center for Natural Products Research and Commercialization, School of Natural Resources and the Environment, College of Agriculture and Life Sciences, University of Arizona, Tucson, AZ 85706-6800, United States

[c]Xenobe Research Institute, P. O. Box 3052, San Diego, CA 92163-1052, United States

Abstract

Access to lead compounds with defined molecular targets continues to be a barrier to the translation of natural product resources. As a solution, we have developed a system that uses discreet, recombinant proteins as the vehicles for natural product isolation. Here, we describe the use of this functional chromatographic method to identify natural products that bind to the AAA+ chaperone, p97, a promising cancer target. Application of this method to a panel of fungal and plant extracts identified rheoemodin, 1-hydroxydehydroherbarin and phomapyrrolidone A as distinct p97 modulators. Excitingly, each of these molecules displayed a unique mechanism of p97 modulation. This discovery provides strong support for the application of functional chromatography to the discovery of protein modulators that would likely escape traditional high-throughput or phenotypic screening platforms.

Keywords

p97/VCP/Cdc48; drug discovery; AAA+; ATPase; natural products

Introduction

The advent of targeted drug therapy emerged with the discovery of Gleevec and was rightly heralded as a major triumph in the pharmaceutical industry.[1] Subsequently, many new targets were brought forth and drug discovery and development strategies emerged leading to many groundbreaking advances in the clinic. However, examination of present

Correspondence to: Eli Chapman, chapman@pharmacy.arizona.edu.

†These authors contributed equally to this work.

Supporting information for this article is available on the WWW under http://www.chembiochem.org or from the author.

discoveries indicates this process is slowing as well as being met with ever increasing costs.[2] Clearly, new tools and procedures are needed to meet these new challenges. To this end, we report a strategy called 'functional chromatography', which offers a general solution to many targeted discovery efforts. To illustrate this procedure, we have chosen the protein quality control machine, p97, which has been touted as a prime target for developing cancer therapeutics.[3] In addition, the highly conserved nature of the ATP-binding domains represents an ongoing conundrum in drug discovery, namely, how to target a specific protein in a family whose members share conserved structure and function.

The biological actions of the AAA+ (ATPase associated with various cellular activities) chaperone p97, also known as Cdc48 or valosin-containing protein (VCP), implicate it in an array of diseases including cancer[4] and neurodegeneration.[4,5] For this reason, a great deal of effort has been put forth to understand p97 function.[6] These studies have ranged from structural investigations to cell-biological studies to genetic dissection to chemical modulation, but many questions remain, especially those that pertain to its physiologic, pathologic, and biochemical function.[7] Moreover, protein quality control machinery has been identified as an effective target for cancer therapeutics, illustrated, in part, by the clinical successes of the proteasome inhibitors Velcade (bortezomib)[8] and Kyprolis (carfilzomib).[9] But given the side effects caused by targeting the proteasome[10] and the rapid appearance of resistance,[11] it has been hypothesized that other, upstream protein quality control machinery may serve as a more suitable target.[12] To this end, we report on a program designed to identify natural products that target p97.

The literature is full of demonstrations of resin supported proteins being used for biological applications including protein purification and analysis of protein-protein interactions, but demonstration of solid supported proteins as a primary vehicle for small molecule isolation has largely evaded examination. Guided by a prior demonstration of reverse-affinity isolation of small molecules to assign a mode of action based on their binding to proteins within cellular proteomes,[13] we worked to develop a procedure to isolate natural products from complex mixtures using a resin-supported target protein. We demonstrate the potential of this technique using p97 as a test case. Using fully functional resin-bound p97, we were able to isolate three natural products from crude extracts, each with a different mechanism of action.

Results and Discussion

Synthesis and characterization of a p97-resin

We began by developing a resin that displayed active, covalently attached p97 protein (Fig. 1a). As p97 operates as a homohexameric ATP-powered machine with many moving parts required for function, our first aim was to discover a resin-based chemistry that would not compromise p97's biochemical activity. After initial screening, we found that purified His_6-tagged p97 was readily loaded on Affi-Gel 15 resin at up to 12 mg/mL. As shown in Fig. 1b, the resin-bound p97 retained its ATPase activity displaying only mild loss of activity as compared to that in solution, which may be due to difficulties with carful quantitation of resin-bound p97 or due to the inhomogeneous nature of the reaction. Because p97 has been shown to hydrolyze ATP only when assembled in the hexameric state,[14] we took this to

indicate the quaternary structure of p97 was intact. Next, we evaluated if the p97-resin was still competent to bind a physiologically relevant co-factor. To this end, the ATPase activity of the resin bound protein was measured in the presence of the trimeric, N-terminal binding p47,[15] a co-factor known to inhibit the ATPase activity of p97,[16] which was observed (Fig. 1c). We further verified p47-binding competence of our p97-resin by determining that [^{35}S]-methionine labeled p47 could be captured selectively from a crude cellular extract (Fig. 1d).

Establishing the functional chromatography workflow

With an active p97-resin in hand, we next screened 880 crude natural product extracts obtained from a diverse collection of microbial and plant species using the work flow illustrated in Fig. 2a. Briefly, 150 μL of p97-resin was incubated with 1 mg/mL of a desired extract for 12 h at 4°C with mutorotation. The resin was pelleted by gentle centrifugation followed by extensive washing and then elution of bound molecules by denaturing the protein. Each of the elution fractions was then analyzed by HPLC and unique peaks subjected to high-resolution mass spectrometry. As a control, we used a resin with no protein (data not shown) or recombinant *E. coli* FtsZ (a protein readily available in our laboratories that served as a non-specific protein control).

Functional chromatographic isolation of rheoemodin (1)

Our first hit was identified from the fungal strain *Chaetomium globosum* isolated from the rhizosphere of the Christmas cactus, *Opuntia leptocaulis* DC (Cactaceae). From this extract, we isolated rheoemodin (**1**),[17] which was enhanced in the p97-resin purified fraction (Fig. 2c) when compared to the parent extract (Fig. 2b). Application of a conventional Malachite green ATPase assay[18] indicated that **1** inhibited the ATPase activity of p97 with an IC_{50} value of 39.8 ± 12.6 μM. As shown in Fig. 2d, **1** was also obtained when using FtsZ-resin, suggesting that **1** may lack specificity.

Isolation of hydroxydehydroherbarin (2) via functional chromatography in the presence of ATP

We also found additional anthraquinone motifs including, 1-hydroxydehydroherbarin (**2**),[19] from an extract of an endolichenic fungus *Corynespora s*p., as illustrated in Figs. 3a–3d. Compound **2** inhibited the ATPase activity of p97 with an IC_{50} value of 21.7 ± 2.2 μM. While these observations provided an initial validation for the method, the fact that **2** did not appear in the protein binding controls (Fig. 3d *versus* Fig. 3b) indicated selective isolation by the p97-resin. Interestingly, however, the isolation of **2** demonstrated that the addition of p97 substrates such as ATP could be used directly to modulate the systems ability to isolate leads, as we observed no detectable binding of **2** in the absence of ATP (Fig. 3c).

Functional chromatographic isolation of phomapyrrolidone A (3)

An extract from the endophytic fungal strain, *Phoma sp*. NRRL 4675, returned a bound fraction that contained two major peaks (Fig. 4b) relative to the crude extract (Fig. 4a) or the control FtsZ-resin (Fig. 4d). We then determined that one of these peaks (highlighted in Fig.

4a–4d) corresponded to phomapyrrolidone A (**3**).[20] After HPLC purification (Fig. 4c), the structure of **3** was confirmed by spectroscopic analyses (see Supporting Information).

Biochemical validation of 1–3 as p97 modulators

To validate biochemical activity of compounds **1**–**3**, we first carried out 12-point dose-responses to study the effect on ATPase activity. All measurements were carried out in a 96-well plate using 50 nM p97 hexamer in 50 mM Tris, 150 mM KCl, 10 mM $MgCl_2$, 1 mM DTT, pH 7.4. Compounds **1**–**3** were added in 12 point dilution (see Supporting Information) and incubated at 21 °C for 10 min followed by addition of 100 μM ATP to initiate the reaction. After 30 min, 60 min, 90 min, or 120 min, aliquots were quenched in malachite green solution and the OD_{670} was measured (see Supporting Information). The IC_{50} value for **3** was determined from these data to be 6.6 ± 0.1 μM (Fig. 5a). To determine if **1**–**3** were competitive-like for the ATP-binding pocket, we inspected the dose-response at 100 μM, 500 μM and 1 mM ATP (Fig. 5a) and found that **1** displayed ATP competitive-like inhibition, **2** was non-competitive, and **3** displayed a complex pattern but was not obviously competitive-like.

Compounds 1–3 show specificity for p97 relative to other ATPases

To test specificity, we measured the activity of **1**–**3** relative to related enzymes (Fig. 5b). First, we determined the activity against a cysteine-less p97 variant, p97-Cys0. Interestingly, the activity of **2** and **3** were effectively unchanged relative to wt-p97, but **1** showed no activity against p97-Cys0. Thinking this might indicate a covalent interaction, we incubated p97 in the presence of 1 mM **1** for 12 h at 4°C, 6 h at 21°C, or 2 h at 37°C. This was followed by extensive dialysis to remove non-covalently bound **1** and residual p97 activity was evaluated by the measurement of ATPase activity. To our surprise, we observed no indication of a covalent modification, as all activity was recovered post-dialysis, relative to a DMSO control. This was interpreted to mean the binding site for **1** is altered by mutation of the cysteine, but for steric reasons and not chemical reasons. Next, to study specificity, we looked at inhibition of three related ATP-utilizing macromolecular machines, the chaperonin, GroEL;[21] the type I AAA+ chaperone, ClpX;[22] and the type II AAA+ *N*-ethylmaleimide sensitive factor (NSF).[23] Remarkably, **1**–**3** showed p97 specificity, but the high specificity relative to NSF was surprising, as this protein is thought to have the highest structural and functional homology to p97.

Measurement of ERAD and UFD using a cell-based assay

Next, we determined the effects of **1**–**3** in cell-based assays using HEK293 cells stably expressing $Ub^{G76V}GFP$[24] or TCRα-GFP[25] (Fig. 6a) to report on the ubiquitin fusion degradation (UFD) pathway and the endoplasmic reticulum associated protein degradation (ERAD) pathway, respectively. As tabulated (Figs. 6b–6c), lack of GFP degradation, indicating p97 function is blocked, in the presence of **1**–**3** was to the same or greater extent than the synthetic quinazolines, DBeQ[26] and ML240.[27] The combination of these data with *in vitro* analyses confirms inhibition of p97 *in vitro* and in cells.

Compounds 1–3 block p97 specific aspects of protein quality control

We then looked at the p97 specificity of **1**–**3** in a cellular context. To start, we determined the cytotoxicity of **1**–**3** in the HEK293 cell line (see Supporting Information). We used this information to identify concentrations that were not cell lethal but offered p97 modulation (concentrations used in Fig. 7). We then looked at total ubiquitylated proteins, which are expected to be elevated in the case of p97 inhibition, as was observed in a dose dependent manner for **1**–**3** (Fig. 7). To differentiate between p97 dependent and p97 independent proteasome mediated degradation, we looked at TCRα-GFP and HA-CD3δ levels by Western blot. TCRα-GFP has been shown to have two major products in cells treated with the proteasome inhibitor, MG132, and one major band in the presence of p97 inhibitors. The lower band that accumulates with proteasomal inhibition is proposed to be a deglycosylated form of TCRα.[27,28] As shown in Fig. 7, treatment with **1**–**3** resulted in a dose-dependent increase in the levels of the upper band, but did not attenuate the lower band. In contrast, MG132, a proteasome inhibitor, led to a dramatic increase in the deglycosylated form of TCRα (Fig. 7). HA-CD3δ is another ER associated protein, but exposes a greater cytosolic portion, thus it can be readily degraded by the proteasome independent of p97.[29] Thus HA-CD3δ levels should be insensitive to p97 inhibition, but not to proteasomal inhibition. As shown, the level of HA-CD3δ did not change as a function of p97 inhibition, but increased dramatically in the presence of MG132. These collective data argue for p97 as the predominant UFD-related target.

Compounds 1–3 induce the UPR, lead to compromised autophagy, and result in apoptosis in a dose dependent manner

Finally, we looked at p97-modulated pathways, which have been correlated with both siRNA knockdown of p97 and chemical inhibition.[27–30] First, we examined the unfolded protein response (UPR). We evaluated all three arms of the UPR and discovered both the PERK and IRE1 arms were activated as demonstrated by dose-dependent increases in phosphorylated eIF2α (p-eIF2α) and the spliced form of Xbp1 (Xbp1s), respectively. Presently, we are unsure why the ATF6 arm is not activated, but we observed no activation of this arm (data not shown). Second, we looked at the effect on autophagy. As expected for p97 inhibitors, the maturation of autophagosomes to autolysosomes was blocked, as indicated by a dose-dependent accumulation of LC3-II (lower band, Fig. 7). Last, we investigated the effects of **1**–**3** on apoptosis by looking at the status of caspase 3 (c-3, Fig. 7). In cells treated with **1**, the concentrations used were below its EC_{50} value, so we did not observe apoptosis. In cells treated with **2**, we saw a potent, dose-dependent increase in caspase 3 levels. In cells treated with **3**, we observed a quite modest apoptotic induction, at the highest concentration, as this is just at the EC_{50} value for this molecule. Taken together, these data argue the molecules in question inhibit the p97 arm of protein quality control, yet do so via discreet mechanisms of action.

Conclusion

Herein, we report three natural products **1**–**3** that modulate p97 function. This discovery was made using functional chromatography on complex extracts, a procedure that selects for binding of a molecule to a protein independent of biochemical function. The molecules

reported varied in potency and mechanism of action, indicating the power of this technique. Compound **1** showed moderate, competitive-like inhibition (sensitive to ATP concentration) and high selectivity against other ATPases, but bound to the FtsZ control resin and did not inhibit p97-Cys0. Compound **2** delivered non-competitive, allosteric inhibition, required ATP to bind to resin-bound p97 (indicating an ATP-induced structural change, which revealed a latent binding pocket), and displayed good p97 selectivity. Compound **3** provided a more complex mechanism with a moderate, but reproducible shift in IC_{50} value at 500 μM ATP with a return to lower values at 1 mM ATP, but also bound to p97-resin in the absence of ATP.

Finally, we validated the potency and selectivity of **1**–**3** in a series of cell-based assays designed to probe two of the prominent p97 protein quality control pathways (UFD and ERAD), the specificity in the UFD, and the effects on p97 modulated functions (UPR, autophagy, and apoptosis). These investigations reveal **1**–**3** as specific molecules for p97 modulation in the UFD pathway. They also show that each of these molecules can, in part, recapitulate siRNA studies. This discovery not only suggests **1**–**3** as leads for further therapeutic evaluation, but also, provides a platform for the discovery of additional natural product leads by adapting recombinant proteins as vehicles for isolation. Overall this study shows that functional chromatography offers a practical and feasible technique to expedite lead identification, a topic of interest to the drug discovery community at large.

Experimental Section

This section contains methods for the key experiments performed. For a complete description of all experiments and spectral data, please see Supplementary Methods.

p97-Cys0

Site directed mutagenesis was performed using wild type pET14b-p97 as a template. Ten of the 12 cysteine residues in p97 (C69, C77, C104, C174, C184, C415, C535, C572, C691, and C695) were mutated to valine and the remaining 2 cysteine residues (C209 and C522) were mutated to alanine or serine using a modified quick change procedure.[31] All mutations were confirmed by DNA sequencing. Expression and purification of the p97-Cys0 protein was carried out as for wt-p97.

Preparation of p97-resin

An aliquot (300 μL) of Affi-Gel 15 resin (Bio-Rad) was washed with H_2O (3 × 300 μL) followed by addition of a 5 mg/mL solution of p97 (300 μL), which was incubated on a LabQuake inversion rotator (Barnstead/Thermolyne) at 4°C. p97-resin coupling efficiency was evaluated by Bradford assay of the supernatant and the resin collected by gentle centrifugation (1000 × g, 1 min) once an $OD_{595} < 0.01$ was reached. The resin was washed with (3 × 500 μL) phosphate buffered potassium chloride (PBK) (50 mM KPhos, 150 mM KCl, pH 7.4).

ATPase assay on resin

The p97-resin (~1 μM p97 hexamer) was suspended in 50 μL of p97 storage buffer (20 mM HEPES, 150 mM KCl, 25 mM $MgCl_2$, 5% glycerol, 2 mM BME, pH 7.4) followed by 5 mM ATP to initiate the reaction. A similar sample with p97 (non-resin bound) in storage buffer was simultaneously examined. At 10 min, 20 min, 30 min, or 40 min, 10 μL aliquots were removed and quenched in 800 μL malachite green solution (9.3 μM malachite green, 53 mM $(NH_4)_2MoO_4$, 1M HCl, 10% Tween 20) for 1 min followed by addition of 100 μL 34% sodium citrate. The OD_{660} was measured using a Genesis 10S UV-Vis Spectrophotometer (Thermo Scientific). The amount of inorganic phosphate (P_i) was determined from a standard curve and plotted as a function of time. Data from this study are provided in Fig. 1b.

ATPase assay in the presence of p47

The p97-resin (~1 μM p97 hexamer) was suspended in 50 μL of p97 storage buffer containing 3.3 μM p47 monomer, followed by 5 mM ATP to initiate the reaction. The rate of ATP hydrolysis was determined as above and the percent activity was calculated and plotted. Data from this study are provided in Fig. 1c.

Affinity capture of [^{35}S]-p47 from a cellular extract. E. coli

BL21(DE3) cells transformed with a p47 expression plasmid were grown in LB (20 mL) with 100 μg/mL of ampicillin until OD_{600} value of 0.6. The culture was then centrifuged (1500 × g for 10 min), gently resuspened in 20 mL of GMML (glycerol based minimal media supplemented with leucine), and incubated for 5 min. Protein expression was then induced with 0.5 mM IPTG in the presence of 60 μL (100 μCi) of [^{35}S]-methionine for 4 h at 37°C. Cells were pelleted by centrifugation (1500 × g for 10 min), resuspended in 500 μL of lysis buffer (50 mM HEPES, 150 mM KCl, 5 mM $MgCl_2$, 5% glycerol, pH 7.4) supplemented with lysozyme (3 mg), incubated on ice for 30 min, and sonicated with a 5 sec pulse/10 sec pause cycle three times. Cell lysates were cleared by centrifugation (16,000 × g for 15 min at 4°C). The soluble fraction was collected and incubated with 1 mL of resin bearing 10 mg/mL p97 for 30 min at 21°C. The resin mixture was washed three times with wash buffer (50 mM HEPES, pH 7.4, 150 mM KCl, 5 mM $MgCl_2$, 5% glycerol). Bound p47 was then eluted by addition 8 M urea (200 μL). The fractions were run on a 12% SDS PAGE gel. The gel was exposed for 18 h on a phosphorimaging casette, and images were collected on a Storm 840 phosphorimager (GE Healthcare). Data from this study are provided in Fig. 1d.

Functional chromatography

A solution of crude extract (1 mg/mL) in PBK (1 mL) was added to 150 μL of resin bearing 5 mg/mL of p97 in a 2 mL Eppendorf tube and mixed on an inversion rotator at 4°C. After 12 h, the supernatant was discarded and the resin washed three times with 500 μL of PBK. After the third wash, bound molecules were eluted with 95% EtOH. The EtOH fraction was transferred to a glass vial, dried by airflow, and analyzed via HPLC followed by high-resolution mass spectrometry (HRMS). Control experiments were run using resin bearing 5 mg/mL of FtsZ.

Supplementary Material

Refer to Web version on PubMed Central for supplementary material.

Acknowledgments

This work was supported by start-up funds provided by the University of Arizona, National Institute of Environmental Health Sciences RO1 ES023758 (E.C.), National Cancer Institute Grant R01 CA90265 (A.A.L.G.), National Cancer Institute R01 CA154377 (D.D.Z.), and National Institute of Environmental Health Sciences ES006694 (a center grant).

References

1. Goldman JM, Melo JV. N. Engl. J. Med. 2003; 349:1451–1464. [PubMed: 14534339]
2. Dickson M, Gagnon JP. Discov. Med. 2004; 4:172–179. [PubMed: 20704981]
3. Valle CW, Min T, Bodas M, Mazur S, Begum S, Tang D, Vij N. PLoS One. 2011; 6:e29073. [PubMed: 22216170]
4. a) Chapman E, Fry AN, Kang M. Mol. Biosyst. 2011; 7:700–710. [PubMed: 21152665] b) Fessart D, Marza E, Taouji S, Delom F, Chevet E. Cancer Lett. 2013; 337:26–34. [PubMed: 23726843] c) Tang WK, Xia D. J. Struct. Biol. 2012; 179:83–92. [PubMed: 22579784] d) Yamanaka K, Sasagawa Y, Ogura T. Biochim. Biophys. Acta. 2012; 1823:130–137. [PubMed: 21781992]
5. Stolz A, Hilt W, Buchberger A, Wolf DH. Trends Biochem. Sci. 2011; 36:515–523. [PubMed: 21741246]
6. a) Liu Y, Ye Y. Curr. Protein. Pept. Sci. 2012; 13:436–446. [PubMed: 22812527] b) Bug M, Meyer H. J. Struct. Biol. 2012; 179:78–82. [PubMed: 22450227]
7. a) Meyer H, Bug M, Bremer S. Nat. Cell Biol. 2012; 14:117–123. [PubMed: 22298039] b) Halawani D, Latterich M. Mol. Cell. 2006; 22:713–717. [PubMed: 16793541]
8. a) Gräwert MA, Groll M. Chem. Commun. 2012; 48:1364–1378.b) Goldberg AL. J. Cell Biol. 2012; 12:583–588. [PubMed: 23148232]
9. Kim KB, Crews CM. Nat. Prod. Rep. 2013; 30:600–604. [PubMed: 23575525]
10. a) Beck P, Dubiella C, Groll M. Biol. Chem. 2012; 393:1101–1120. [PubMed: 23091276] b) Cvek B. Prog. Mol. Biol. Transl. Sci. 2012; 109:161–226. [PubMed: 22727422]
11. a) Cao B, Li J, Mao X. Curr. Pharm. Des. 2013; 19:3190–3200. [PubMed: 23151134] b) Ruschak AM, Slassi M, Kay LE, Schimmer AD. J. Natl. Cancer Inst. 2011; 103:1007–1017. [PubMed: 21606441] c) Mujtaba T, Dou QP. Discov. Med. 2011; 12:471–480. [PubMed: 22204764]
12. a) Hjerpe R, Rodríguez MS. Int. J. Biochem. Cell Biol. 2008; 40:1126–1140. [PubMed: 18203645] b) Nalepa G, Wade-Harper J. Cancer Treat. Rev. 2003; 29(Suppl. 1):49–57. [PubMed: 12738243] c) Nalepa G, Rolfe M, Wade-Harper J. Nat. Rev. Drug Discov. 2006; 5:596–613. [PubMed: 16816840]
13. a) Rodríguez AD, Lear MJ, La Clair JJ. J. Am. Chem. Soc. 2008; 130:7256–7358. [PubMed: 18479102] b) La Clair JJ, Rodríguez AD. Bioorg. Med. Chem. 2011; 19:6645–6653. [PubMed: 21784648] c) Lear MJ, Simon O, Foley TL, Burkart MD, Baiga TJ, Noel JP, DiPasquale AG, Rheingold AL, La Clair JJ. J. Nat. Prod. 2009; 72:1980–1987. [PubMed: 19842686]
14. a) Niwa H, Ewens CA, Tsang C, Yeung HO, Zhang X, Freemont PS. J. Biol. Chem. 2012; 287:8561–8570. [PubMed: 22270372] b) Briggs LC, Baldwin GS, Miyata N, Kondo H, Zhang X, Freemont PS. J. Biol. Chem. 2008; 283:13745–13752. [PubMed: 18332143] c) Wang Q, Song C, Li CH. Biochem. Biophys. Res. Commun. 2003; 300:253–260. [PubMed: 12504076]
15. a) Kondo H, Rabouille C, Newman R, Levine TP, Pappin D, Freemont P, Warren G. Nature. 1997; 388:75–78. [PubMed: 9214505] b) Dreveny I, Kondo H, Uchiyama K, Shaw A, Zhang X, Freemont PS. EMBO J. 2004; 23:1030–1039. [PubMed: 14988733]
16. a) Bruderer RM, Brasseur C, Meyer HH. J. Biol. Chem. 2004; 279:49609–49616. [PubMed: 15371428] b) Meyer HH, Kondo H, Warren G. FEBS Lett. 1998; 437:255–257. [PubMed: 9824302]

17. Wijeratne EMK, Turbyville TJ, Fritz A, Whitesell L, Gunatilaka AA. Biorg. Med. Chem. 2006; 14:7917–7923.

18. Chapman E, Farr GW, Fenton WA, Johnson SM, Horwich AL. Proc. Natl. Acad. Sci. U S A. 2008; 105:19205–19210. [PubMed: 19050077]

19. a) Wijeratne EMK, Bashyal BP, Gunatilaka MK, Arnold AE, Gunatilaka AAL. J. Nat. Prod. 2010; 73:1156–1159. [PubMed: 20521776] b) Paranagama, Wijeratne EMK, Burns AM, Marron MT, Gunatilaka MK, Arnold AE, Gunatilaka AAL. J. Nat. Prod. 2007; 70:1700–1705. [PubMed: 17988097]

20. Wijerante EMK, He H, Franzblau SG, Hoffman AM, Gunatilaka AAL. J. Nat. Prod. 2013; 76:1860–1865. [PubMed: 24079882]

21. Horwich AL, Fenton WA, Chapman E, Farr GW. Annu. Rev. Cell. Dev. Biol. 2007; 23:115–145. [PubMed: 17489689]

22. Baker TA, Sauer RT. Biochim. Biophys. Acta. 2012; 1823:15–28. [PubMed: 21736903]

23. Zhao C, Smith EC, Whiteheart SW. Biochim. Biophys. Acta. 2012; 1823:159–171. [PubMed: 21689688]

24. a) Hamer G, Matilainen O, Holmberg CI. Nat. Methods. 2010; 7:473–478. [PubMed: 20453865] b) Stack JH, Whitney M, Rodems SM, Pollok BA. Nat. Biotechnol. 2000; 18:1298–1302. [PubMed: 11101811]

25. Schleicher U, Röllinghoff M, Gessner A A. J. Immunol. Methods. 2000; 246:165–174. [PubMed: 11121557]

26. Chou TF, Brown SJ, Minond D, Nordin BE, Li K, Jones AC, Chase P, Porubsky PR, Stoltz BM, Schoenen FJ, Patricelli MP, Hodder P, Rosen H, Deshaies RJ. Proc. Natl. Acad. Sci U S A. 2011; 108:4834–4839. [PubMed: 21383145]

27. Chou TF, Li K, Frankowski KJ, Schoenen FJ, Deshaies RJ. Chem Med Chem. 2013; 8:297–312. [PubMed: 23316025]

28. Wójcik C, Rowicka M, Kudlicki A, Nowis D, McConnell E, Kujawa M, DeMartino GN. Mol. Biol. Cell. 2006; 17:4606–4618. [PubMed: 16914519]

29. Yu H, Kopito RR. J. Biol. Chem. 1999; 274:36852–36858. [PubMed: 10601236]

30. Magnaghi P, D'Alessio R, Valsasina B, Avanzi N, Rizzi S, Asa D, Gasparri F, Cozzi L, Cucchi U, Orrenius C, Polucci P, Ballinari D, Perrera C, Leone A, Cervi G, Casale E, Xiao Y, Wong C, Anderson DJ, Galvani A, Donati D, O'Brien T, Jackson PK, Isacchi A. Nat. Chem. Biol. 2013; 9:548–556. [PubMed: 23892893]

31. Zheng L, Baumann U, Reymond JL. Nucleic Acids Res. 2004; 32:e1152.

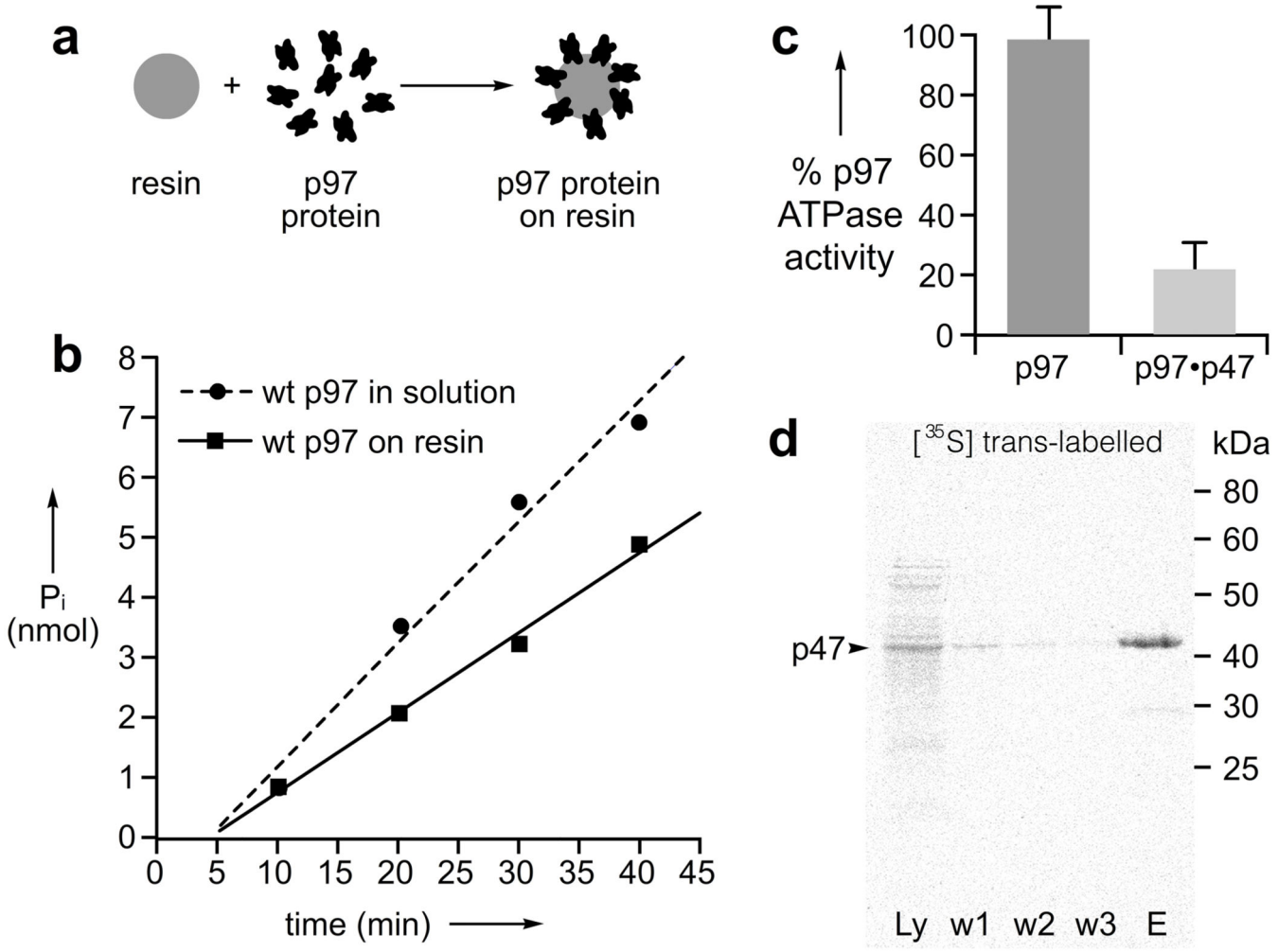

Figure 1.

p97 retains biochemical function when displayed on resin. **a)** Schematic representation of the loading of p97 on resin. **b)** ATPase analysis indicates that Affi-Gel 15 resin bearing p97 at a final solution concentration of 1 μM hexamer displays comparable activity as 1 μM p97 hexamer in 20 mM HEPES, 150 mM KCl, 25 mM $MgCl_2$, 2 mM BME, 5% glycerol, 5 mM ATP, pH 7.4. **c)** Co-factor-binding is maintained as demonstrated by the reduction in p97's ATPase activity upon adding 3.3 μM p47 monomer to resin bearing 1 μM p97 hexamer. **d)** p97-resin can specifically capture p47 from a cell extract. The five lanes are given as follows: **Ly** – crude lysate, **w1–w3** – three independent washes, and **E** – denaturing elution. Samples were separated by 12% SDS-PAGE and visualized with a phosphorimager.

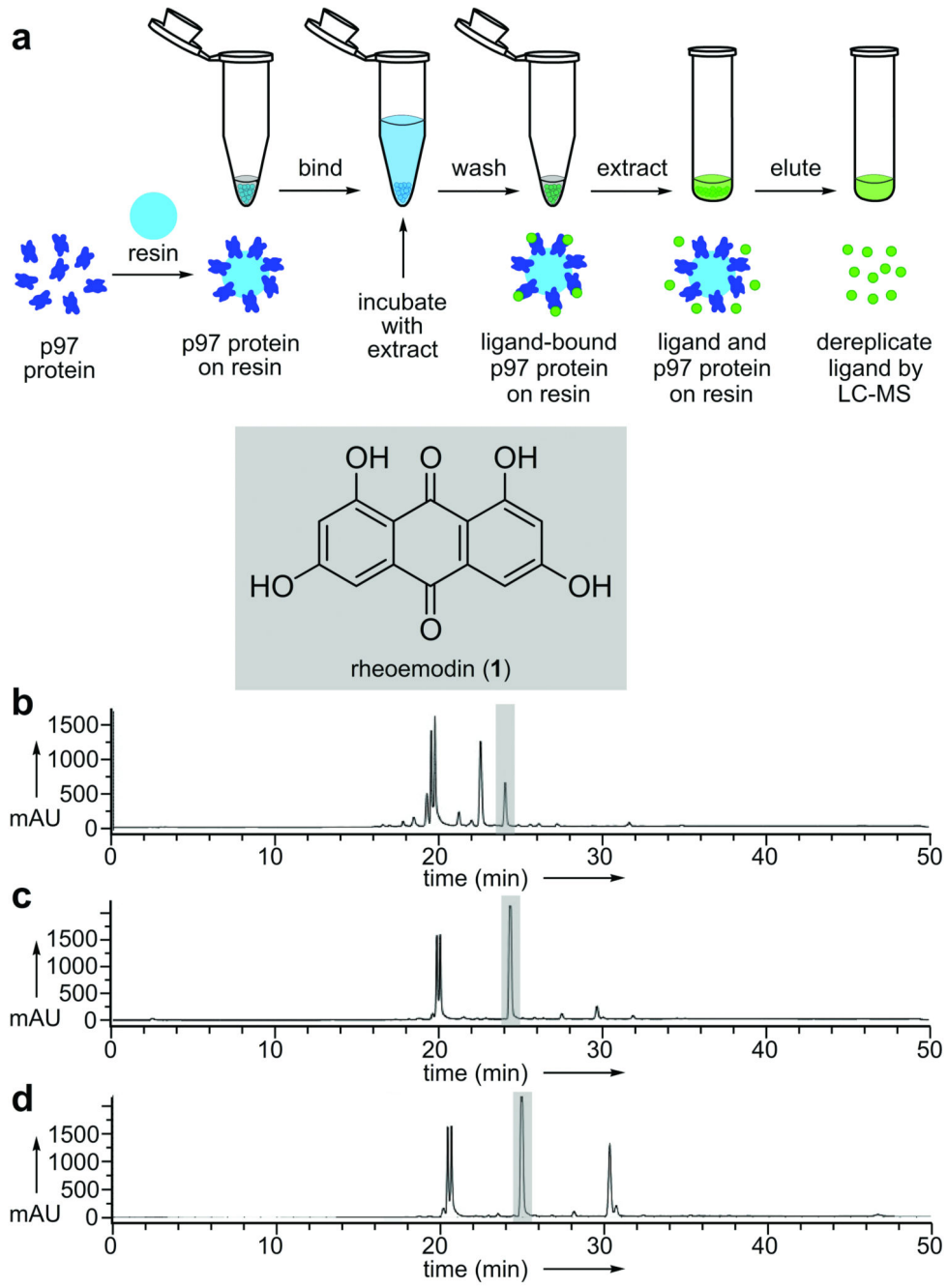

Figure 2.

Functional chromatographic isolation of rheoemodin (**1**) from extracts of a *C. globosum* culture. **a)** A schematic representation depicting the steps involved in isolating p97 binding molecules from crude natural product extracts. **b)** HPLC trace of the *C. globosum* extract. **c)** HPLC trace collected after application of 150 μL of resin bearing 5 mg/mL of p97 to 1 mg of *C. globosum* extract in 1 mL of PBK buffer (50 mM KPhos, 150 mM KCl, pH 7.4). **d)** HPLC trace collected after application of 150 μL of resin bearing 5 mg/mL of FtsZ (protein binding control) to 1 mg of *C. globosum* extract in 1 mL of PBK.

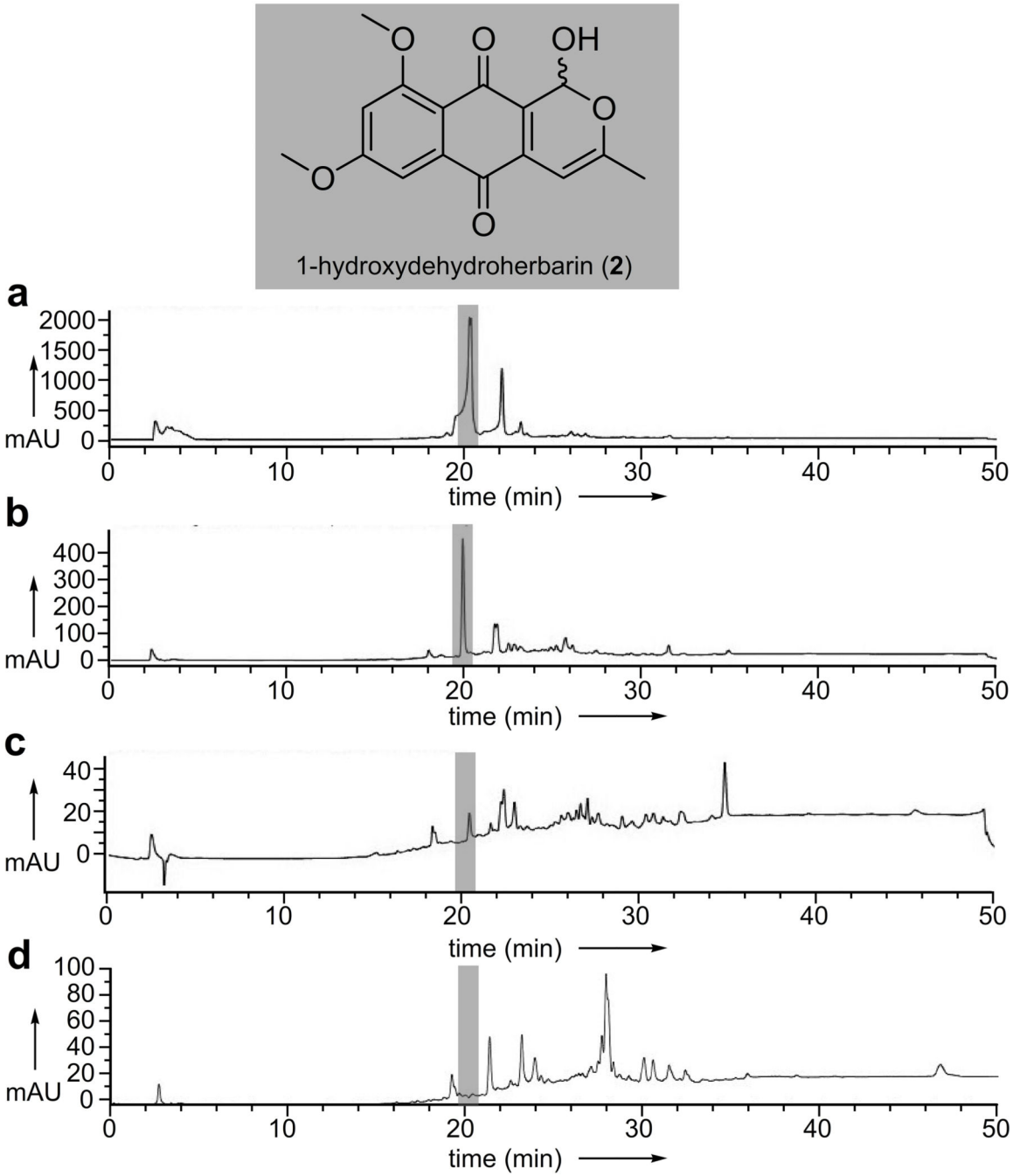

Figure 3.

Functional chromatographic isolation of 1-hydroxydehydroherbarin (**2**) from an extract of a *Corynespora sp*. **a)** HPLC trace of the *Corynespora sp.* extract. **b)** HPLC trace collected after application of 150 μL of resin bearing 5 mg/mL of p97 to 1 mg of *Corynespora sp.* extract in 1 mL of PBK containing 100 μM ATP. **c)** HPLC trace collected after application of 150 μL of resin bearing 5 mg/mL of p97 to 1 mg of *Corynespora sp.* extract in 1 mL of PBK (without ATP). **d)** HPLC trace collected after application of 150 μL of resin bearing 5

mg/mL of FtsZ (protein binding control) to 1 mg of *Corynespora sp.* extract in 1 mL of PBK.

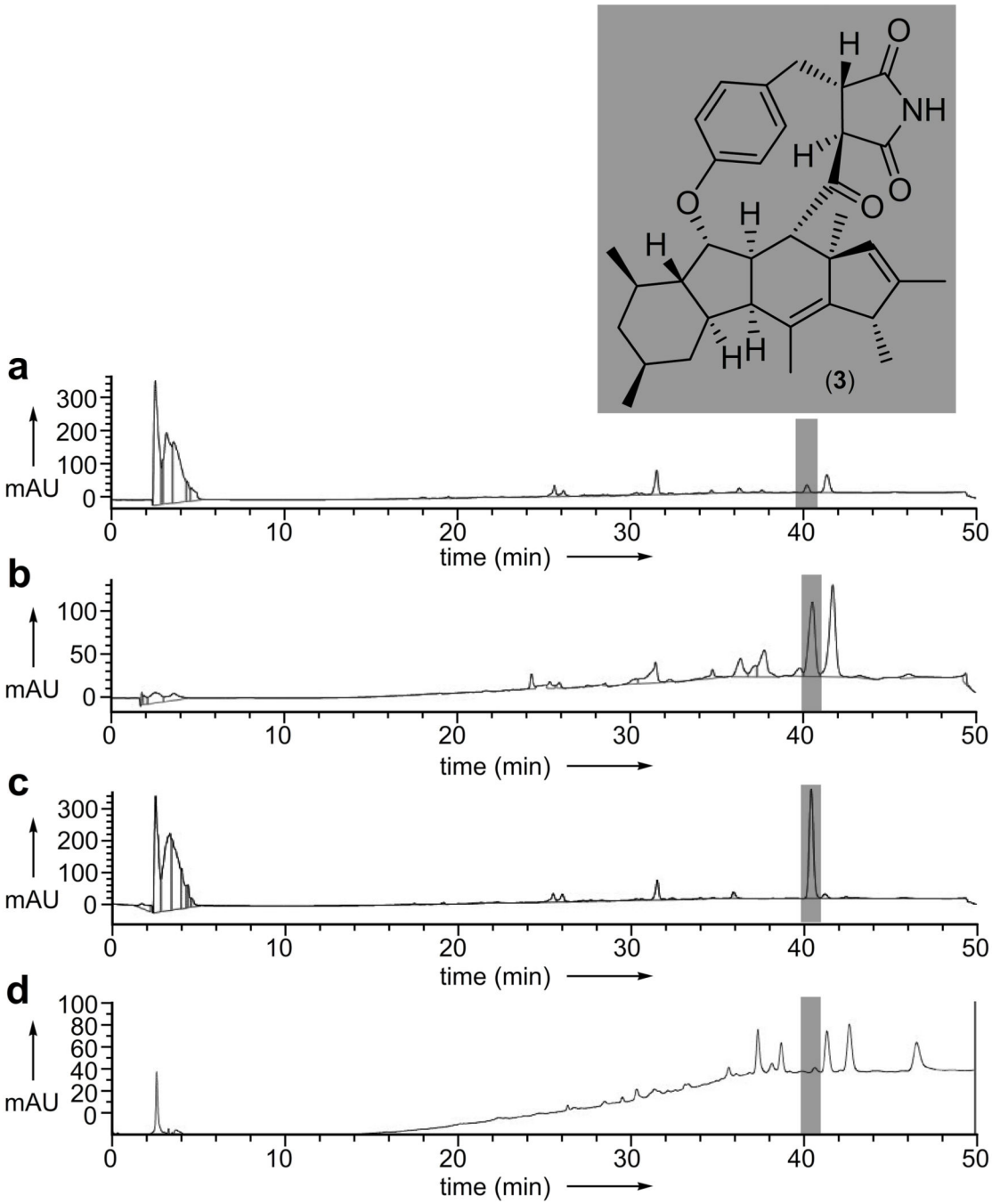

Figure 4.

Functional chromatographic isolation of phomapyrrolidone A (**3**) from an extract of *Phoma sp.* NRRL 4675 using a p97-resin. **a)** HPLC trace of the *Phoma sp.* NRRL 4675 extract. **b)** HPLC trace collected after application of 150 μL of resin bearing 5 mg/mL of p97 to 1 mg of *Phoma sp.* NRRL 4675 extract in 1 mL of PBK. **c)** HPLC trace of purified **3**. **d)** HPLC trace collected after application of 150 μL of resin bearing 5 mg/mL of FtsZ (protein binding control) to 1 mg of *Phoma sp.* extract in 1 mL of PBK.

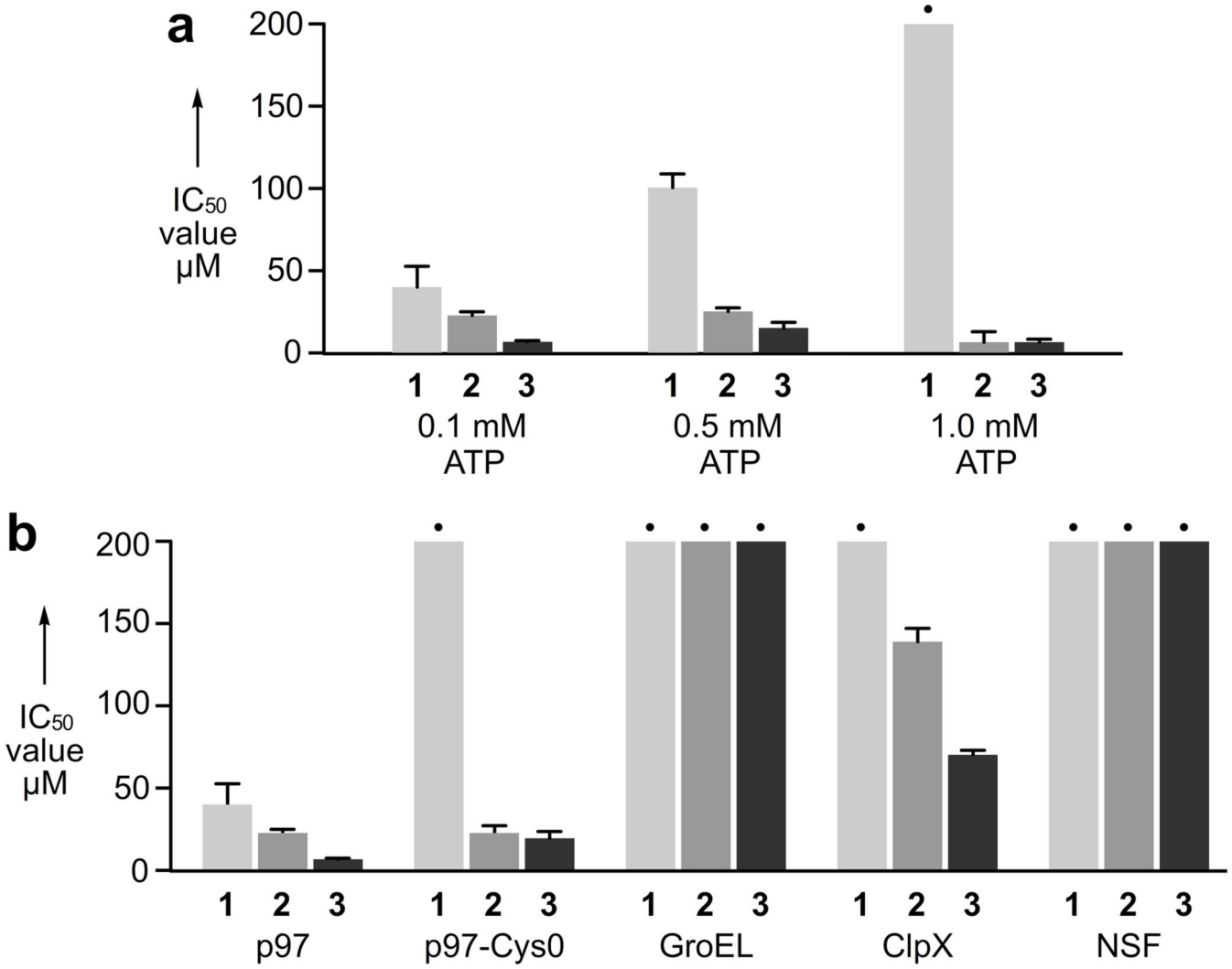

Figure 5.

Biochemical activity and ATPase selectivity of compounds **1**–**3**. **a)** IC_{50} values of **1**–**3** at increasing ATP concentrations. **b)** Compounds **1**–**3** effects on p97-Cys0 or other ATP-utilizing machines. • indicates values that were > 200 μM.

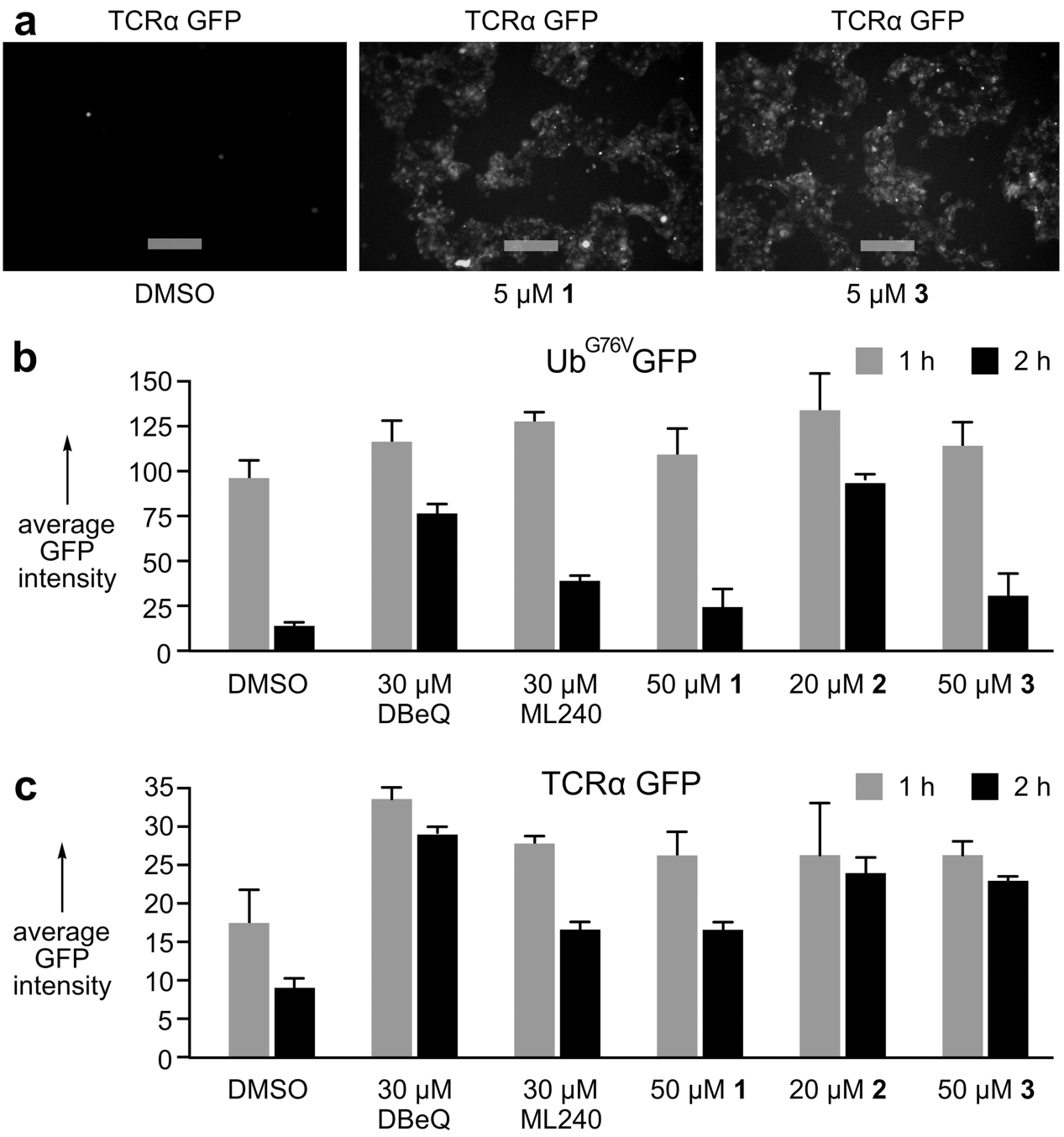

Figure 6.

Validation of activity in cells. **a**) Fluorescence microscopy images of HEK293 cells expressing TCRα-GFP, a reporter of ERAD function. Cells treated with **1** or **3** prevented p97-mediated TCRα-GFP degradation, while rapid degradation occurred in the DMSO (negative) control. Images were collected by excitation at 488 nm and emission at 510 nm. Bars denote 10 μm. **b**) Quantitation of HEK293 cells expressing $Ub^{G76V}GFP$, a UFD reporter. **c**) Quantitation of HEK293 cells expressing TCRα-GFP. Average GFP intensity

represents an average fluorescence observed per cell for ~10,000 events examined relative HEK293 cells lacking a GFP reporter (non-fluorescent blank) at 0.

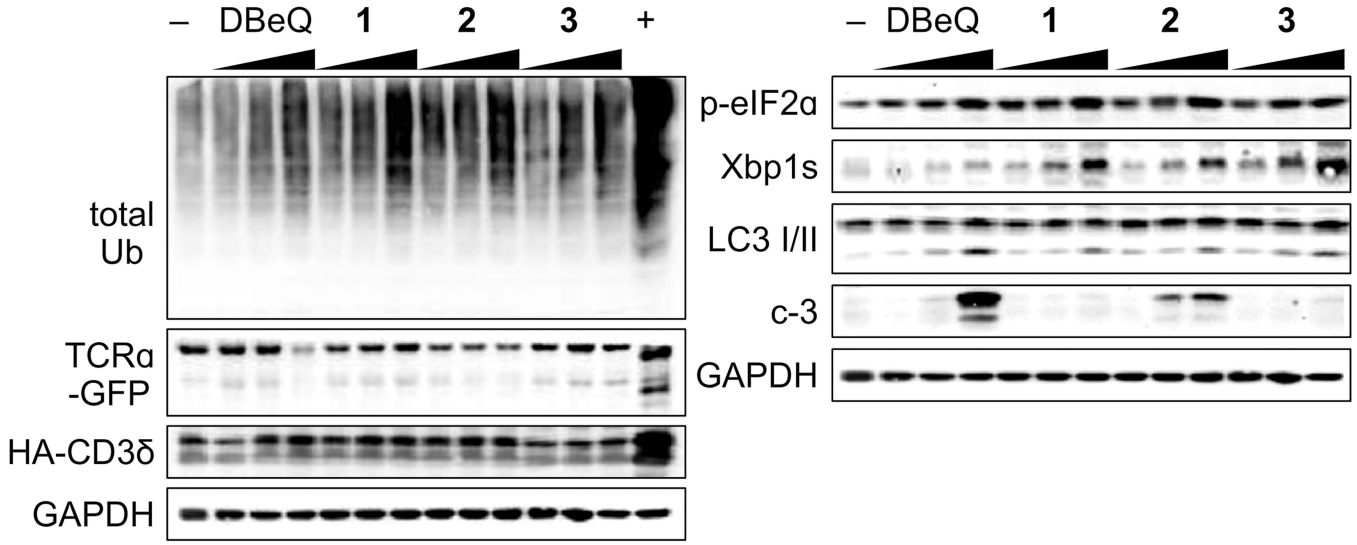

Figure 7.

Western blot analysis depicting the levels of total ubiquitylation (total Ub), TCRα-GFP, HA-CD3δ, p-eiF2a, Xbp1s, LC3 I/II, caspase 3 (c-3) in HEK293 cells treated with either 10 μM, 20 μM, or 50 μM **1** (EC_{50} value of 113.0 ± 1.2 μM); 1 μM, 5 μM, or 10 μM **2** (EC_{50} value of 2.1 ± 0.3 μM) or 1 μM, 10 μM, or 20 μM **3** (EC_{50} value of 20.2 ± 0.5 μM); or 5 μM, 10 μM, and 15 μM for DBeQ. Cells were treated the ascribed compound for 24 h at 37 °C. The negative control (−) was treated with 0.1% DMSO and the positive control (+) with 5 μM MG132. GAPDH was used as a loading control.